Cues from neuroepithelium and surface ectoderm maintain neural crest-free regions within cranial mesenchyme of the developing chick

Development 129, 1095-1105 (2002)
Printed in Great Britain © The Company of Biologists Limited 2002
DEV2728

Cues from neuroepithelium and surface ectoderm maintain neural crest-free regions within cranial mesenchyme of the developing chick

Jon P. Golding*, Monica Dixon and Martin Gassmann*

Division of Neurobiology, National Institute for Medical Research, The Ridgeway, London NW7 1AA, UK
*Authors for correspondence (e-mail: jgoldin@nimr.mrc.ac.uk and martin.gassman@unibas.ch)

Accepted 14 December 2001

SUMMARY

Within the developing vertebrate head, neural crest cells (NCCs) migrate from the dorsal surface of the hindbrain into the mesenchyme adjacent to rhombomeres (r)1 plus r2, r4 and r6 in three segregated streams. NCCs do not enter the intervening mesenchyme adjacent to r3 or r5, suggesting that these regions contain a NCC-repulsive activity.

We have used surgical manipulations in the chick to demonstrate that r3 neuroepithelium and its overlying surface ectoderm independently help maintain the NCC-free zone within r3 mesenchyme. In the absence of r3, subpopulations of NCCs enter r3 mesenchyme in a dorsolateral stream and an ectopic cranial nerve forms between the trigeminal and facial ganglia. The NCC-repulsive activity dissipates/degrades within 5-10 hours of r3 removal. Initially, r4 NCCs more readily enter the altered mesenchyme than r2 NCCs, irrespective of their maturational stage. Following surface ectoderm removal, mainly r4 NCCs enter r3 mesenchyme within 5 hours, but after 20 hours the proportions of r2 NCCs and r4 NCCs ectopically within r3 mesenchyme appear similar.

Key words: Chick, Neural crest cells, Mesenchyme, Surface ectoderm, Migration, Patterning

INTRODUCTION

Within the developing vertebrate head, the organisation of skeletal structures and peripheral nerves depends on the orchestrated migration of pluripotent cranial neural crest cells (NCCs) through the cranial mesenchyme (Bronner-Fraser, 1995; Le Douarin, 1982). Cranial NCCs are generated throughout the dorsal hindbrain (Sechrist et al., 1993) but their emigration into the adjacent mesenchyme is patterned from the outset into three distinct streams (Lumsden et al., 1991) that mirror the transient segmentation of the neural tube into lineage-restricted units, called rhombomeres (r) (Lumsden and Krumlauf, 1996; Trainor and Krumlauf, 2000a). Thus, only at the level of r1+r2, r4 and r6 do NCCs migrate into the cranial mesenchyme. Fewer NCCs leave r3 and r5, owing to increased cell death (Graham et al., 1996), and they do not exit laterally, directly into the mesenchyme, but instead migrate rostrally and caudally along the dorsal surface of the neural tube to join NCCs in the neighbouring even-numbered rhombomeres (Kulesa and Fraser, 1998; Sechrist et al., 1993). After leaving the neural tube, NCCs still avoid entering r3 and r5 mesenchyme, suggesting that the cranial mesenchyme is segmented molecularly, as no anatomical segmentation has been observed (Freund et al., 1996). The idea that NCC 'exclusion zones' exist within the mesenchyme adjacent to r3 and r5 is supported by experiments demonstrating that quail cranial NCCs grafted into chick cranial mesenchyme migrate only into host mesenchyme adjacent to even-numbered rhombomeres (Farlie et al., 1999). The generation of NCC 'exclusion zones' may depend on cues from r3 and r5 neuroepithelium and/or on interactions among the NCCs themselves. In ovo grafting experiments to alter relative positions of rhombomeres and mesenchyme (Kuratani and Eichele, 1993; Sechrist et al., 1994) provide evidence for cues from neuroepithelium, while dorsal hindbrain ablation studies (Kulesa et al., 2000) suggest a role for NCC cell-cell interactions.

Although the origins, migration pathways and destinations of cranial NCCs are well documented (Koentges and Lumsden, 1996; Lumsden et al., 1991), relatively few molecules have been found that influence their pathfinding. These include specific ephrins and their Eph receptors (Adams et al., 2001; Helbling et al., 1998; Holder and Klein, 1999; Robinson et al., 1997; Smith et al., 1997), Collapsin 1 (Eickholt et al., 1999), FGF2 (Kubota and Ito, 2000) and an uncharacterised chemoattractant released from the otic vesicle (Sechrist et al., 1994). Where studied in vivo, these factors appear to be involved in maintaining the segregation of NCC streams at the level of the branchial arches. However, the cues that enforce NCC segregation further dorsally, adjacent to the neuroepithelium, remain unknown.

In this study, we show that cues from r3 neuroepithelium and the overlying surface ectoderm are required to exclude subpopulations of NCCs from r3-adjacent mesenchyme.

MATERIALS AND METHODS

Embryos

Fertilised hens' eggs were from Winter Egg Farm, Hertfordshire. Quail eggs were from Birkbeck College, London. Eggs were incubated at 38±1°C until the embryos had 9-16 pairs of somites (ss).

Surgery

Eggs were 'windowed' (Mason, 1999) and finely drawn glass needles were used for surgery. For neuroepithelial ablation, the left half of r3 was freed from surrounding tissue by incisions made just lateral to the rhombomere, along its mid-line, and along the r3/4 and r3/2 boundaries. For surface ectoderm ablation, a rectangle was cut superficially into the surface ectoderm, which was then carefully peeled off. The incisions extended from the dorsal mid-line laterally through 90 degrees, while along the AP axis they extended into the neighbouring r2 and r4 ectoderm by up to half a segment.

Cell tracing and cell grafting

For tracing migrating cells a 3 mg/ml solution of DiI or DiO (D-282, D-275; Molecular Probes) in dimethylformamide was microinjected into dorsal r2 or r4.

For cell grafting experiments, r2 or r4 were cleanly removed from donor embryos and labelled for 3 minutes with 250 μg/ml CM-DiI (C-7000, Molecular Probes) dissolved in Tyrode's solution containing 5% ethanol, 5% sucrose and 25% foetal calf serum. Labelled rhombomeres were washed with Tyrode's solution before either grafting into host embryos or dissecting the dorsal half into smaller fragments for injection into dorsal r2 or r4 of host embryos. After labelling, host r3 or r3 surface ectoderm were unilaterally removed. Embryos were allowed to develop for a further 5-45 hours.

Axon tracing

Forty-five hours after r3 removal, embryos were fixed in 4% paraformaldehyde in phosphate-buffered saline (PBS). DiI (3 mg/ml in dimethylformamide) was injected bilaterally into r2 or r4 basal plate, or into the ectopic cranial nerve. Embryos were viewed 3 days later.

In situ hybridisation

Whole-mount in situ hybridisation (Grove et al., 1998) was performed using 1 μg/ml digoxigenin-labelled riboprobe at 70°C. Chick *Hoxb1*, *Hoxa2* and *EphA4* plasmids were gifts from Robb Krumlauf. Chick *Sox10* plasmid was a gift of Paul Scotting and Yi-Chuan Cheng.

Immunohistochemistry

Whole-mount immunohistochemistry (Lumsden and Keynes, 1989) was performed using anti-HNK1 (clone VC1.1; C0678, Sigma; 1:100), anti-neurofilament-160 kDa (clone RMO-270; Zymed Laboratories; 1:500) or anti-quail antibodies (Q¢PN; gift of Andrew Lumsden; 1:4). Anti-mouse Ig secondary antibodies were HRP or Cy3 conjugated (Amersham; 1:300).

RESULTS

Removal of r3 leads to altered migration of neural crest cells

In initial experiments the alar plate of r3 was excised unilaterally in 9ss-14ss embryos and the migration pattern of NCCs was revealed either by HNK-1 immunohistochemistry (Fig. 1A-C) or *Sox10* in situ hybridisation (Fig. 1D-F) after 20 hours in ovo. HNK-1 recognises a cell-surface carbohydrate on NCCs (Holley and Yu, 1987), while *Sox10* is expressed by migrating neurogenic NCCs (Cheng et al., 2000).

Both markers revealed the normal pattern of pre-otic NCC migration on the unoperated side of all embryos. This consisted of two segregated streams of NCCs, emerging from r1+r2 [migrating ventrally towards the first branchial arch (ba1) and more rostrally], and from r4 [migrating ventrally towards the second branchial arch (ba2)] (Fig. 1B,E). [Note that NCCs within ba1 and ba2 are mainly chondrogenic and do not express *Sox10* (Cheng et al., 2000).] On the operated side of the same embryos, in addition to the normal patterns of NCC migration, a discrete band of ectopic NCCs extended through the mesenchyme adjacent to the removed r3 (r3*) at the dorsoventral level of the otic vesicle (Fig. 1A,D). The extent of the observed phenotype depended on the method of NCC detection. *Sox10* riboprobe normally revealed a robust aberrant stream of NCCs extending through lateral r3* mesenchyme,

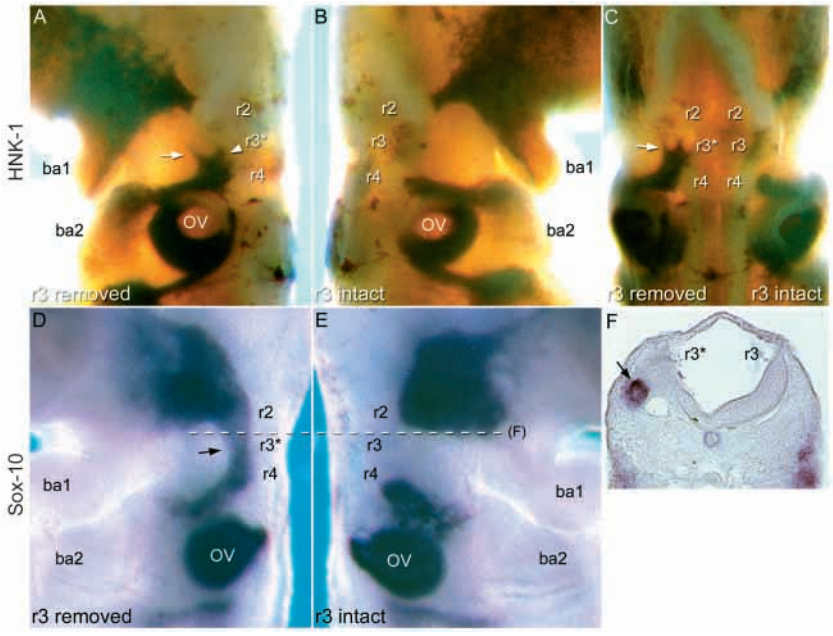

Fig. 1. Altered pattern of cranial NCC migration 20 hours after unilateral r3 removal. (A-C) Whole-mount HNK-1 immunostaining of NCCs showing the operated (A) and unoperated (B) sides of the same embryo. (C) Dorsal view. (D-F) *Sox10* in situ hybridisation to show migrating NCCs on the operated (D) and unoperated (E) sides of the same embryo. (F) A transverse section through the embryo at the level of r3 that corresponds to the broken line in D,E. On the operated side, in addition to the normal pattern of NCC migration (r2 crest migrates into ba1; r4 crest migrates into ba2), a stream of NCCs (arrow in A,C,D,F) migrates aberrantly through the mesenchyme adjacent to the removed r3 (r3*). This ectopic NCC stream is more clearly defined by *Sox10* mRNA expression than by HNK1 immunoreactivity. In addition, HNK1^{+} cells are detected within the space previously occupied by r3 (arrowhead in A). ba1 and ba2, branchial arches 1 and 2; OV, otic vesicle.

usually connecting the r4 and r2 NCC streams (arrow in Fig. 1D,F) (12/24 embryos). This NCC bridge was seldom seen in embryos stained with HNK1 antibody, which more frequently revealed a rostrally tapering projection of NCCs from the r4 NCC stream into r3* mesenchyme (arrow in Fig. 1A,C) and a projection of NCCs from r4 neuroepithelium into r3* (arrowhead in Fig. 1A) (5/11 embryos). This difference between *Sox10* expression and HNK1 staining might reflect differentiation of the ectopic NCCs. Chick cranial NCCs normally maintain HNK-1 immunoreactivity upon differentiation, but their behaviour in the unfamiliar environment of r3* mesenchyme may well differ. In control experiments, where r3 was unilaterally removed and then replaced, no changes in the pattern of NCC migration were detected after 20 hours with *Sox10* probe (14 embryos) or HNK1 antibody (seven embryos) (not shown).

In subsequent r3 removal experiments, the full dorsoventral extent of r3 was excised unilaterally in 9ss-11ss embryos. This was found to be technically more reproducible and resulted in a higher proportion of embryos with the aberrant *Sox10*$^+$ NCC migration phenotype (47/52 embryos after 20 hours). To investigate the origins of the misguided NCCs and to monitor the progression of the phenotype, we injected a fluorescent dye (DiI) into left dorsal r4 or r2, to label pre-migratory NCCs, just prior to r3 removal on the left side. The distribution of migrating DiI-labelled cells was examined at 5, 10, 20 and 30 hours post-surgery and compared with the distribution of *Sox10*-expressing NCCs in the same embryos (Fig. 2). In embryos where r4 was DiI labelled, large numbers of DiI-labelled NCCs migrated into ba2 within 5 hours, although in only 4/17 embryos did cells migrate aberrantly into r3* mesenchyme (arrow in Fig. 2B). In addition, several r4-derived cells entered r3*, the gap left in the neuroepithelium after removing r3 (arrowhead in Fig. 2B). However, *Sox10* riboprobe labelled no cells within r3* or r3* mesenchyme at 5 hours postsurgery (Fig. 2C, although DiI$^-$/Sox10$^+$ cells were sometimes found in association with the dorsal surface ectoderm). Only by 10 hours after surgery could a distinct subpopulation of r4-derived NCCs be detected within r3* mesenchyme (11/14 embryos), as revealed both by DiI labelling (Fig. 2D,E) and *Sox10* in situ hybridisation (Fig. 2F; aberrant cells indicated by an arrow in Fig. 2E), although *Sox10* was not detectable in all DiI-labelled ectopic cells (arrowhead in Fig. 2E). We do not know the identity of the *Sox10*$^-$/DiI$^+$ cells. By 20 hours postsurgery a bridge of aberrantly migrating r4-derived cells connected the r4 and r2 NCC streams (23/29 embryos) and some r4-derived cells could be detected within the r2 NCC stream (Fig. 2G-I). By this stage, the distributions of DiI-labelled cells and *Sox10*-expressing cells coincided within r3* mesenchyme. Similarly, at 30 hours postsurgery, aberrantly migrating DiI$^+$/*Sox10*$^+$ r4-derived NCCs were detected within r3* mesenchyme and now also within the developing trigeminal ganglion (Fig. 2J-L) (11/12 embryos). Occasionally, DiI-labelled cells were also seen in ba1 (data not shown).

In a separate series of experiments, r2 cells were DiI labelled just prior to unilateral r3 removal. By 10 hours postsurgery r2-derived DiI-labelled cells were found within r3*, but none were detected within r3* mesenchyme (eight embryos, not shown). By 20 hours postsurgery r2-derived DiI-labelled cells were occasionally seen within r3* mesenchyme (8/44 embryos) (Fig. 2M-O), but the aberrant cells were always fewer in number than had been seen with labelled r4 cells at 20 hours. By contrast, at 30 hours post-surgery, labelled r2 cells were often detected within r3* mesenchyme (8/12 embryos) and within the facial ganglion (Fig. 2P-R). Perhaps there are repellents preferentially affecting r2 NCCs that take longer to dissipate from r3* mesenchyme than r4-preferential NCC repellents do. Alternatively, the r2 cells might be migrating along the already-formed ectopic NCC bridge. To study cell migration at later time points, we homotopically bilaterally grafted 10ss quail r2 or r4 into 10ss chick embryos, unilaterally removed r3 and visualised the distribution of donor quail cells 72 hours later with quail-specific antibody (10 embryos each condition). Ectopic quail cells were detected only on the operated side of grafted embryos. Ectopic quail r2 cells were found within an ectopic cranial nerve between the trigeminal and facial ganglia (see Fig. 6) and within the facial ganglion itself (Fig. 2S), but not within ba2 (Fig. 2T,U). Ectopic quail r4 cells were found within the ectopic cranial nerve and trigeminal ganglion (Fig. 2V) and also ba1 (Fig. 2W,X). Although r2 and r4 NCCs contribute to distinct jaw structures (Koentges and Lumsden, 1996), we detected no craniofacial abnormalities in r3 ablated embryos after 7 days using Alcian Blue (data not shown), suggesting that ectopic cells eventually die or change their identity.

In summary, although cells from both r2 and r4 rapidly repopulate the acellular region of r3*, the NCC population that migrates aberrantly into r3* mesenchyme initially comprises mainly r4-derived NCCs, and these aberrant NCCs only begin to leave their normal migratory pathway between 5 and 10 hours after r3 removal. The reluctance of NCCs to enter r3* mesenchyme immediately after surgery argues against this aberrant migration being a nonspecific injury-induced effect and is instead consistent with the continued presence of a repulsive activity within r3* mesenchyme for the first few hours after r3 removal.

Heterotopic grafting reveals intrinsic differences in the responsiveness of r2 NCCs and r4 NCCs to r3* mesenchyme

The observation that predominantly r4 NCCs initially migrate aberrantly into r3* mesenchyme might relate to intrinsic differences between r2 NCCs and r4 NCCs, or to local differences in the mesenchymal environment. In order to differentiate between these possibilities, we performed unilateral heterotopic transplantations of either entire DiI-labelled rhombomeres or of small clusters of DiI-labelled dorsal neuroepithelium (containing pre-migratory NCCs) followed by unilateral removal of host r3. Ten hours after surgery, we found that when r2 was unilaterally grafted in place of r4, DiI-labelled r2 NCCs migrated along the appropriate (r4) pathway for their new location, but seldom migrated rostrally into r3* mesenchyme (in only 4/11 embryos; Fig. 3A-C). However, when r4 unilaterally replaced r2, DiI-labelled r4 NCCs migrated along the r2 pathway but many cells also deviated caudally into r3* mesenchyme (in 7/10 embryos; Fig. 3E-G). In control experiments, where rhombomeres were transplanted but r3 was left intact, no aberrant NCC migration was observed (four embryos each; not shown).

To determine whether transplanted rhombomeres maintained their identity, we performed *Hoxb1* in situ

hybridisation, as , in the chick, *Hoxb1* is expressed by r4 but not r2 (Maden et al., 1991). In agreement with Guthrie (Guthrie et al., 1992), we found that r4 maintained *Hoxb1* expression in the r2 position (Fig. 3H), while r2 did not markedly express *Hoxb1* in the r4 position (Fig. 3D).

In contrast to the results obtained by transplanting entire rhombomeres, when smaller clusters of r2 cells were grafted into r4, several of the ectopically placed cells migrated rostrally into r3* mesenchyme (in 6/10 embryos; Fig. 3I-K). Conversely, when r4 cells were grafted into r2, the r4-derived cells seldom migrated caudally into r3* mesenchyme (in only 2/12 embryos; Fig. 3M-O). In these embryos we detected no *Hoxb1*-negative r2 cells within r4 neuroepithelium (Fig. 3L) and found very few r4 cells maintaining *Hoxb1* expression within r2 neuroepithelium (Fig. 3P), suggesting that grafted cells may change positional identity to match that of their new environment. In the chick, even-to-even-numbered rhombomere cell transplants become dispersed within the

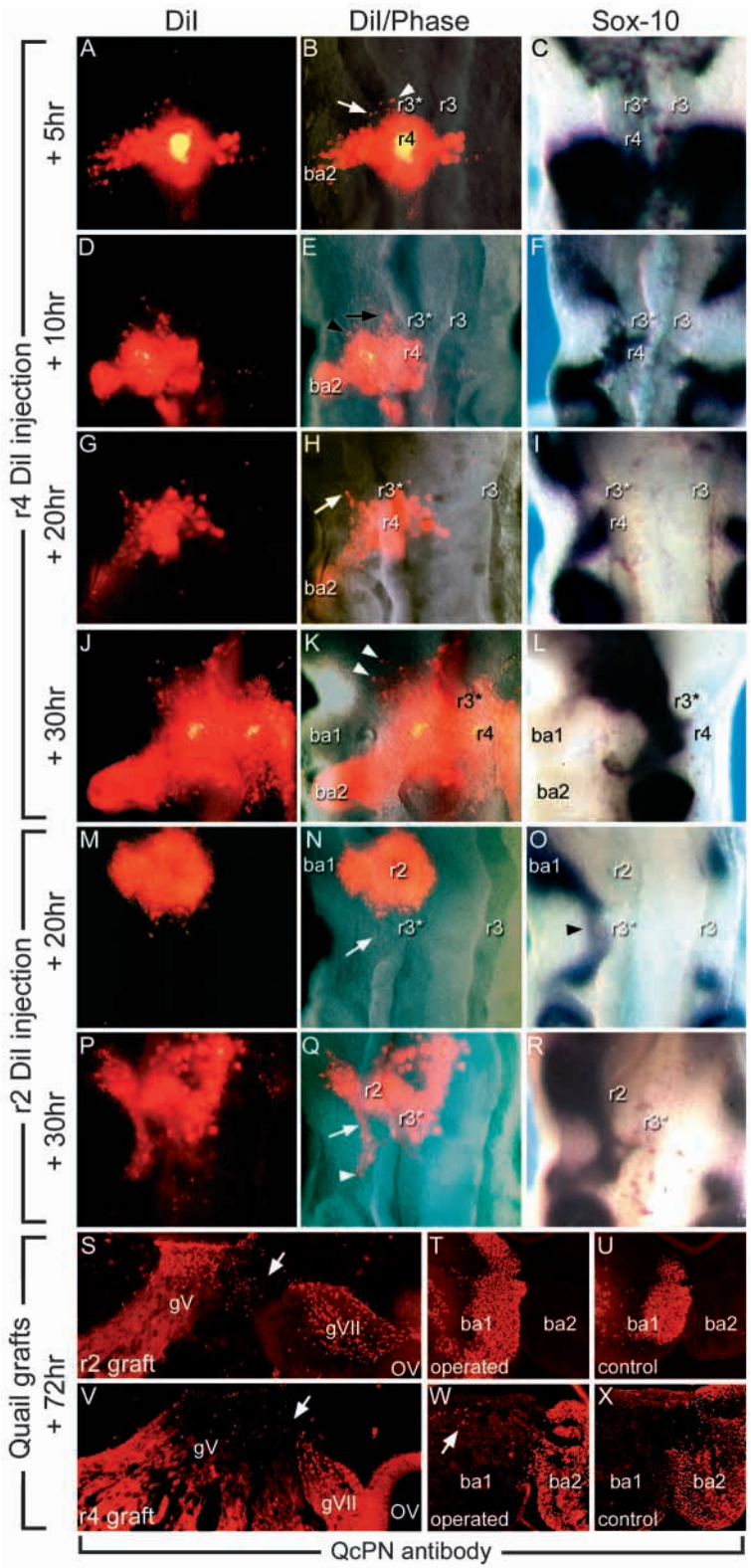

Fig. 2. Time-course and rhombomeric origin of aberrantly migrating NCCs. Before left-side r3 removal, cells in r4 or r2 were marked in one of two ways. In some embryos, cells within dorsal r4 or r2 were labelled by focal DiI injection. These embryos were allowed to develop for a further 5, 10, 20 or 30 hours and processed for *Sox10* in situ hybridisation. In other embryos, r4 or r2 were replaced homotopically with quail rhombomeres. These embryos were allowed to develop for a further 72 hours and processed for anti-Q¢PN immunohistochemistry. (A-C) Dorsal views 5 hours after r3 removal. r4 cells have migrated appropriately towards ba2, while very few cells migrate aberrantly into mesenchyme adjacent to the removed r3 (r3*) (arrow) or directly into the space left by removing r3 (arrowhead). Appropriately migrating r4 cells express *Sox10* (a marker of migrating NCCs), but *Sox10* expression is not detected in aberrantly migrating r4 cells. (D-F) Dorsal views 10 hours after r3 removal. Several r4 cells have now migrated aberrantly into r3* mesenchyme (arrow) and *Sox10* is expressed within proximal r3* mesenchyme. However, some aberrantly migrating r4 cells, more distal to the neuroepithelium, do not express *Sox10* (arrowhead). (G-I) Dorsal views 20 hours after r3 removal. A robust stream of aberrantly migrating r4 cells is present within r3* mesenchyme (arrow) and intersects the stream of neural crest cells from r2. All of the aberrantly migrating r4 cells within r3* mesenchyme now fall within the region of *Sox10* expression. (J-L) Lateral views of operated side 30 hours after r3 removal. Aberrantly migrating r4 cells are within r3* mesenchyme and can be detected within the developing trigeminal ganglion (arrowheads). (M-O) Dorsal views 20 hours after r3 removal. Many r2 cells are migrating appropriately towards ba1, but DiI labelled r2 cells seldom migrate aberrantly into r3* mesenchyme (arrow), even though a robust stream of *Sox10* expressing, aberrantly migrating cells was detected within r3* mesenchyme in these embryos (arrowhead). (P-R) Dorsal views. By 30 hours after r3 removal, r2 cells had migrated into r3* mesenchyme (arrow) and were occasionally seen within the developing facial/acoustic ganglion (arrowhead). (S-X) Sagittal sections of quail-to-chick homotopic r2 or r4 grafts, stained with Q¢PN antibody 72 hours after r3 removal. (S) r2-derived quail cells were located appropriately within the trigeminal ganglion (gV) and ectopically within the facial ganglion (gVII) and the ectopic cranial nerve (arrow). (T-U) Quail r2 cells were not found within ba2 on either the operated (T) or control (U) sides. (V) Quail r4-derived cells were located appropriately within the facial ganglion and ectopically within the trigeminal ganglion and the ectopic cranial nerve (arrow). (W) Quail r4 cells were found ectopically within ba1 (arrow), but were not seen in ba1 on the unoperated side (X). ba1, branchial arch 1; ba2, branchial arch 2.

ectopic neuroepithelial environment (Guthrie et al., 1993), while in the mouse, as engrafted r4 cells disperse within r2 they lose *Hoxb1* expression (Trainor and Krumlauf, 2000b).

Our data reveal intrinsic differences between r2 NCCs and r4 NCCs, and suggest that multiple repulsive cues may exist within r3 mesenchyme. Thus, r2 NCCs are reluctant to enter r3 mesenchyme whether r3 is present or not, while several r4 NCCs enter r3 mesenchyme in the absence of the repulsive cues associated with r3.

After r3 removal, r3* mesenchyme gradually becomes permissive to NCCs

At least two explanations could account for the observed delay of 5 hours between r3 removal and the initial appearance of aberrantly migrating r4 NCCs within r3* mesenchyme. The r3-dependent repulsive activity might disappear rapidly from the mesenchyme after r3 removal, but only late-migrating NCCs might be competent to respond to this changed environment. Alternatively, the repulsive activity might require several hours to dissipate/degrade after r3 removal and the age of the NCCs could be relatively unimportant. To discriminate between these possibilities, we studied the migration of r4 cells in a number of cell tracing/grafting paradigms (summarised in Fig. 4A,B).

In the first paradigm, DiI-labelled dorsal r4 cells were grafted homotopically from 16ss donor embryos into 10ss host embryos (i.e. donor cells 10 hours older than host cells, 18 embryos). Host r3 was unilaterally removed and the migration of DiI-labelled donor cells was examined after 5 hours (Fig. 4A). Under these conditions, donor r4 cells migrated within the normal r4 NCC stream towards ba2, but very few donor r4 cells migrated aberrantly into r3* mesenchyme (Fig. 4C-E), comparable with the situation at 5 hours postsurgery in our original time-course experiments (compare with Fig. 2A,B). To control for the possibility that at low density donor cells might

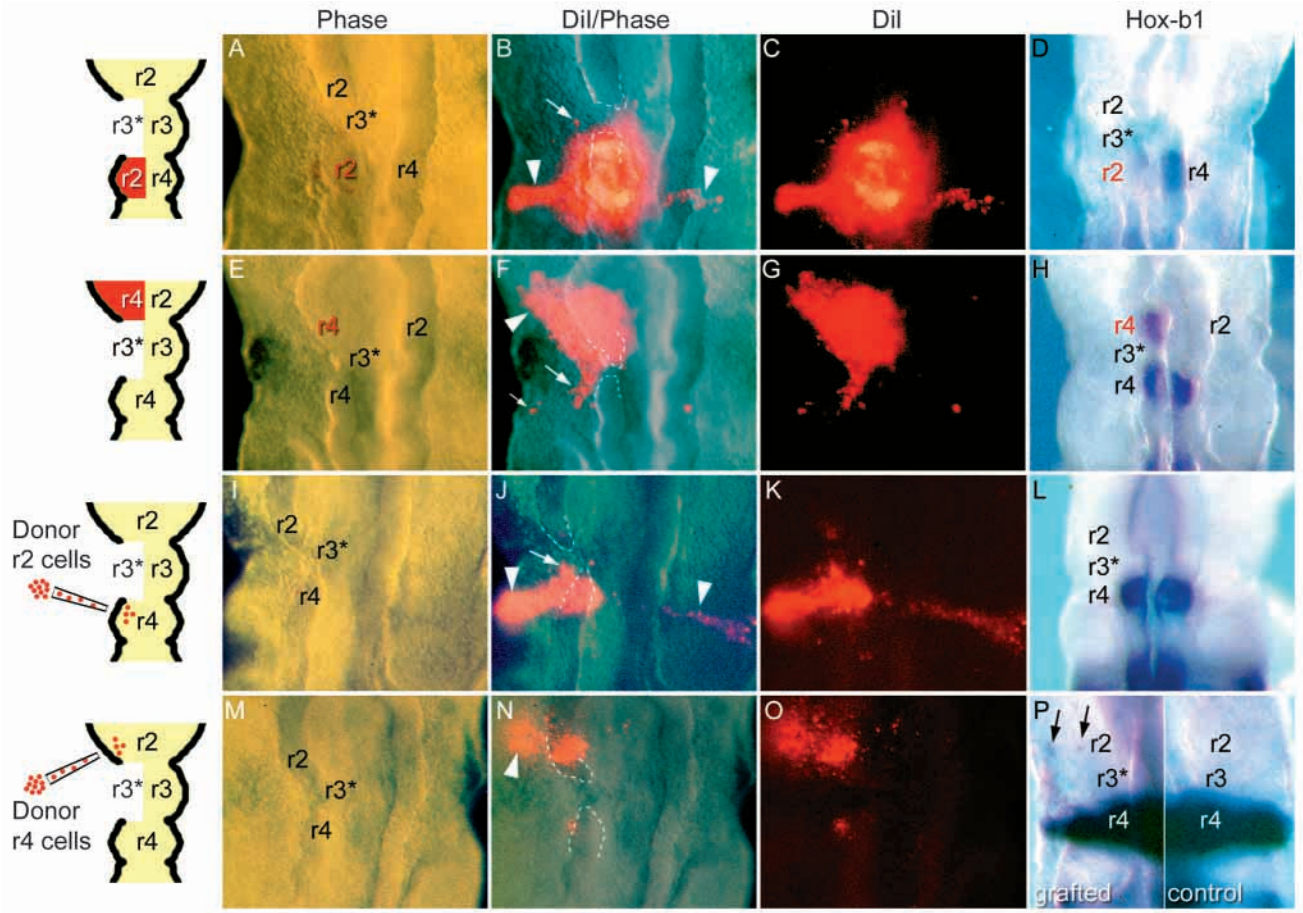

Fig. 3. Heterotopic NCC grafting. Cartoons on the left summarise each experiment, and panels show dorsal views of the distribution of grafted cells 10 hours after surgery. Phase, combined phase/DiI, DiI and Hoxb1 in situ images. Broken lines mark the neuroepithelial outlines. (A-D) Unilaterally, r4 was replaced by DiI-labelled r2, and then r3 was removed. Ectopic r2 cells migrate along the normal r4 NCC pathway (arrowheads), but few cells migrate into r3* mesenchyme (arrow). Ectopic r2 did not express the r4 marker, *Hoxb1* (D). (E-H) Unilaterally, r2 was replaced by DiI-labelled r4, and then r3 was removed. Ectopic r4 cells migrate along the normal r2 NCC pathway (arrowhead) and many cells migrate caudally into r3* mesenchyme (arrow), with some entering the normal r4 NCC pathway (small arrow). Ectopic r4 maintains *Hoxb1* expression (H). (I-P) In similar experiments, small clusters of neuroepithelial cells were heterotopically grafted between r2 and r4. (I-L) Ectopically grafted r2 cells migrate out of r4 within the r4 NCC stream (arrowheads) and several cells migrate rostrally into r3* mesenchyme (arrow). *Hoxb1* expression within r4 appears unaltered. (M-P) Ectopically grafted r4 cells migrate within the r2 NCC stream (arrowhead), but cells rarely deviate caudally into r3* mesenchyme. (P) Grafted and control sides of host hindbrain flatmount, stripped of mesenchyme to aid viewing. Within r2 neuroepithelium, very few grafted r4 cells maintain *Hoxb1* expression (arrows), suggesting that in small clusters, ectopic NCCs lose their original positional identity.

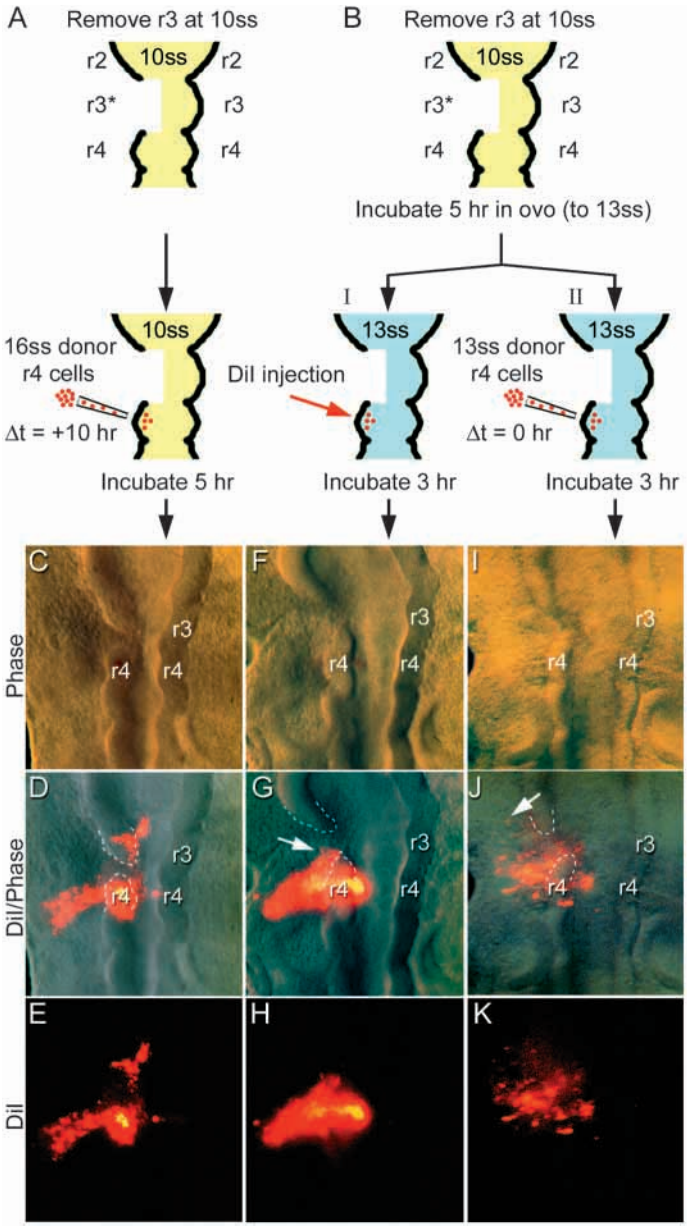

Fig. 4. After r3 removal, r3* mesenchyme gradually loses its NCC repulsive character. Experiments were performed to determine whether maturational changes intrinsic to NCCs (A,C-E), or surgically induced changes within the mesenchyme (B,F-K) were responsible for the observed delay between r3 removal and the onset of the aberrant NCC migration phenotype. Broken lines mark the neuroepithelial outlines. (A) r3 was removed at 10ss, clusters of donor DiI-labelled 16ss r4 cells were grafted homotopically into r4 and the embryos incubated for a further 5 hours. (C-E) Phase, combined phase/DiI, and DiI images, respectively, reveal that grafted cells seldom migrate into r3* mesenchyme, indicating that the r3 mesenchymal repulsive activity persists for up to 5 hours after r3 removal and affects late-migrating NCCs (cluster of cells within r2 in D,E is a cell injection artefact and does not represent migration from r4). (B) r3 was removed at 10ss and embryos were incubated for 5 hours before either directly labelling host r4 cells with DiI (I; F-H) or homotopically grafting age-matched DiI labelled r4 cell clusters (II; I-K). Embryos were then incubated for a further 3 hours. (F-K) Phase (F,I), combined phase/DiI (G,J) and DiI (H,K) images reveal that several r4 cells rapidly migrate (within 3 hours) into rostral r3* mesenchyme (arrows) following this additional post-operative period. This indicates that the mesenchymal repulsive activity is absent within 8 hours of r3 removal.

become changed within the host neuroepithelial environment, we unilaterally replaced 10ss host r4 with 16ss donor r4 and removed r3. These results (10 embryos, not shown) replicated the cell cluster transplant experiments. Thus, a repulsive activity persists in r3* mesenchyme for up to 5 hours postsurgery and later-migrating r4 cells continue to be responsive to this activity.

In the second paradigm, we investigated the role of the environment. We unilaterally removed r3 at 10ss and incubated these embryos for 5 hours (to 13ss). Then host dorsal r4 cells were labelled by DiI injection (Fig. 4B part I; six embryos). After a further 3 hours, we found that labelled r4 cells had migrated in the r4 NCC stream towards ba2 and many labelled r4 cells had also migrated into r3* mesenchyme (Fig. 4F-H). To control for any injury-induced changes in host r4 NCCs, labelled r4 cells from unoperated 13ss donor embryos were grafted homotopically into 13ss host embryos in which r3 had been unilaterally removed at 10ss (Fig. 4B, part II; 10 embryos). The migration of labelled cells was examined 3 hours later. Donor r4 cells migrated in the r4 NCC stream towards ba2 and also into r3* mesenchyme (Fig. 4I-K).

Taken together, these data favour a model in which subsets of r4 cells from a wide age range are sensitive to a repulsive activity that is gradually lost from r3* mesenchyme.

Positional identity markers are unchanged after r3 removal

To determine whether aberrantly migrating r4 NCCs maintain expression of r4 segment identity markers within r3* mesenchyme, we used the r4 marker *Hoxa2*, which is expressed transiently by migrating r4 NCCs, but not by r2 NCCs (Prince and Lumsden, 1994). Pre-migratory r4 NCCs were labelled unilaterally with DiI at 10ss, before unilateral r3 removal, and embryos were processed for *Hoxa2* in situ hybridisation 20 hours later. In cases where a dense stream of DiI-labelled r4 NCCs entered r3* mesenchyme (Fig. 5A,B), this aberrant NCC stream maintained *Hoxa2* expression (Fig. 5C arrow), even within ba1 (Fig. 5C, arrowhead). However, when r4 cells entering r3* mesenchyme were few and dispersed (Fig. 5D,E), *Hoxa2* expression could not be detected in this region (Fig. 5F arrow). This suggests that in the absence of cues from neighbouring r4 NCCs or the appropriate mesenchymal environment, r4 NCCs fail to maintain normal levels of a marker of their original AP identity. This finding is consistent with data from mice that demonstrate the importance of local environmental cues in reinforcing the positional identity of migrating NCCs (Golding et al., 2000; Trainor and Krumlauf, 2000b).

By 45 hours after r3 removal, although *Hoxa2* was still strongly expressed within ba2, no ectopic expression was detected within ba1 (not shown). As our quail graft experiments demonstrated r4 NCCs ectopically within ba1 up to 72 hours after surgery, this suggests that ectopic r4 NCC derivatives adjust their Hox expression in response to their new environment.

Our initial studies demonstrated that cells from r2 and r4 entered r3* (the space previously occupied by r3; see Figs 1

and 2). However, in this ectopic environment, no incoming cells were found to express *Hoxb1*, an r4 neuroepithelial marker (Maden et al., 1991). *Hoxb1* continued to show a sharp limit of expression at the r4/r3* boundary, although the position of r4 on the operated side of embryos often appeared shifted slightly rostrally (Fig. 5G). This suggests that r4 cells that enter r3* are either NCCs that have already downregulated *Hoxb1*, or r4 neuroepithelial cells that downregulate *Hoxb1* in the ectopic r3* environment. Previous work indicates that the cells that infill ablated rhombomeres can readjust their Hox gene expression (Hunt et al., 1995). To further investigate the identity of cells that entered r3* we used an *EphA4* (*Sek*) riboprobe, which identifies r3 and r5 neuroepithelial cells (Nieto et al., 1992). Embryos were processed for *EphA4* in situ hybridisation either immediately after unilateral r3 removal (Fig. 5H), or 20 hours after surgery (Fig. 5I). At neither time point was *EphA4* expression detected within r3*. These data confirm that our surgical procedures cleanly remove r3 and that although cells infiltrate r3* from neighbouring r2 and r4, this does not result in the regeneration of an r3 phenotype. In addition to providing information on cells that re-populate r3*, our results indicate that r4 positional identity markers are not altered by r3 removal.

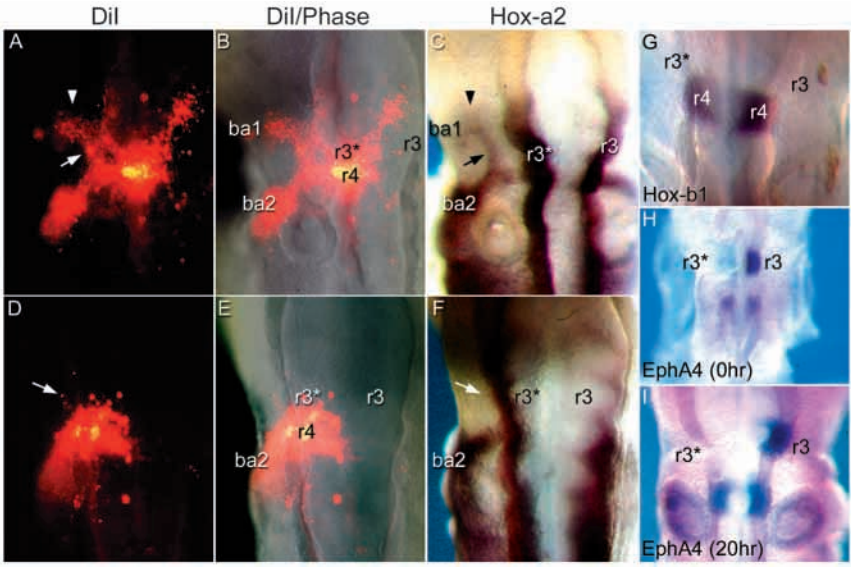

Fig. 5. Following r3 removal, positional identity marker expression is unchanged within the neuroepithelium, but depends on r4 NCC density within r3* mesenchyme. (A-F) Dorsal views of two embryos (A-C and D-F) in which r4 cells were labelled with DiI at the time of r3 removal and the distribution of migrating r4 cells was examined 20 hours later. These embryos were subsequently labelled with *Hoxa2* riboprobe. NCCs from r4 express *Hoxa2* as they migrate along their normal pathway towards ba2 (C,F). (A-C) Under conditions of high density, aberrantly migrating r4 NCCs continue to express *Hoxa2* within r3* mesenchyme (arrows) and even within ba1 (arrowheads). (D-F) However, when relatively small numbers of DiI-labelled r4 cells enter r3* mesenchyme (arrow in D) they no longer maintain *Hoxa2* expression in ectopic locations (arrow in F). (G) *Hoxb1* expression within r4 is unaffected 20 hours after r3 removal and although our previous dye-labelling experiments show that some r4 cells repopulate r3*, we found no evidence of *Hoxb1*-expressing cells within r3*. (H,I) *EphA4* is normally expressed by r3 and r5. Some embryos were processed for *EphA4* in situ hybridisation immediately after r3 removal (0 hours) to demonstrate the clean removal of r3 (H). Other embryos were processed for *EphA4* in situ 20 hours after surgery and demonstrate that none of the cells repopulating r3* express *EphA4* (I). ba1, branchial arch 1; ba2 branchial arch 2.

Axon misprojections following r3 removal

Cranial NCCs give rise to several differentiated cell types, including components of the peripheral nervous system. Therefore, we investigated whether, in addition to aberrant NCC migration, there were any changes in cranial nerve anatomy, after r3 removals.

Neurogenic NCCs from r2 and r4 contribute to the trigeminal ganglion and the facial/acoustic ganglia, respectively. By 20 hours after r3 removal, whole-mount anti-neurofilament antibody staining revealed a small number of axons extending through r3* mesenchyme, between the developing trigeminal ganglion and the facial/acoustic ganglia (Fig. 6A,B). No neuronal cell bodies were detected within r3* mesenchyme and we did not detect any axons entering r3* mesenchyme directly from the lesioned neuroepithelium (Fig. 6A,B). By 30 hours after r3 removal, the number of mis-projecting axons was greater and they had fasciculated into a thin bridge between the trigeminal and facial/acoustic ganglia (Fig. 6D,E). By 45 hours after r3 removal, a substantial ectopic nerve was present between these ganglia (Fig. 6G), which persisted at 72 hours (Fig. 6H).

The origin of axons contributing to the ectopic cranial nerve was investigated by injecting DiI into the nerve 45 hours after r3 removal. Peripherally, axons and neuronal cell bodies within the trigeminal and facial ganglia were labelled (Fig. 6I). Centrally, longitudinally running sensory axons were labelled. Motoneurone cell bodies within r1, r2, r4 and r5 were sometimes labelled (Fig. 6J,K). However, when DiI was applied to medial r2 (Fig. 6L,M) or medial r4 (Fig. 6N,O) (in the vicinity of motoneurones), aberrant axon projections were rarely detected peripherally within r3* mesenchyme after r2 labelling and never after r4 labelling.

Removal of r3 surface ectoderm also alters NCC migration pathways

Two distinct cell types abut the cranial mesenchyme. Medially, it contacts neuroepithelium, while laterally it contacts surface ectoderm. In order to investigate the contribution that surface ectoderm-derived cues might make to cranial NCC pathfinding, we unilaterally removed r3 surface ectoderm and examined the distribution of *Sox10*-expressing cells 20 hours later. Similar to the r3 removal phenotype, we detected a cohort of *Sox10*-expressing cells extending through r3 mesenchyme (Fig. 7A-D; 15/39 embryos).

The progression of this phenotype and the source of the ectopic cells was studied by DiO labelling of r2 and DiI labelling r4, unilaterally removing r3 surface ectoderm and examining the migration of dye-labelled cells, together with the distribution of *Sox10*-expressing NCCs after 5 and 10 hours. The onset of aberrant cell migration occurred sooner

after surface ectoderm removal than had been seen with r3 removals. Thus, after 5 hours, some DiI$^+$ r4 cells migrated into r3 mesenchyme (6/11 embryos), while fewer DiO$^+$ r2 cells less frequently entered r3 mesenchyme (3/11 embryos) (Fig. 7E,F). Correspondingly, at 5 hours we detected only aberrant rostral migration of *Sox10*$^+$ r4 NCCs into r3 mesenchyme (3/6 embryos) (Fig. 7G). By 10 hours, many DiI$^+$ r4 cells entered r3 mesenchyme (5/9 embryos), although the proportion and frequency of DiO$^+$ r2 cells within r3 mesenchyme remained lower (3/9 embryos) (Fig. 7H,I). By 10 hours, a bridge of *Sox10*$^+$ NCCs often extended through r3 mesenchyme (5/6 embryos, Fig. 7J). Separate r2 DiI-labelling and r4 DiI-labelling experiments were performed for the 20 hour time point (Fig. 7M-R), by which time r3 mesenchyme contained similar proportions of r2-derived cells (4/5 embryos) and r4-derived cells (5/6 embryos). Dye-labelled cells remained more widely dispersed within r3 mesenchyme than did *Sox10*-expressing NCCs (compare Fig. 7Q with 7R). DiI labelling of r3 rarely revealed direct emigration of cells into r3-adjacent mesenchyme 20 hours after ectoderm removal (1/6 embryos, not shown). By labelling the cranial surface ectoderm with a droplet of DiI, before removing r3 surface ectoderm, we determined that ectodermal cells do not repopulate r3 mesenchyme within 5 hours (not shown) but some do by 10 hours (10 embryos each) (Fig. 7K,L) and several by 20 hours (8 embryos) (Fig. 7S,T). Therefore, we cannot exclude the possibility that the scattered dye-labelled, *Sox10*$^-$ cells within r3 mesenchyme at 10 and 20 hours could be of ectodermal origin rather than NCCs.

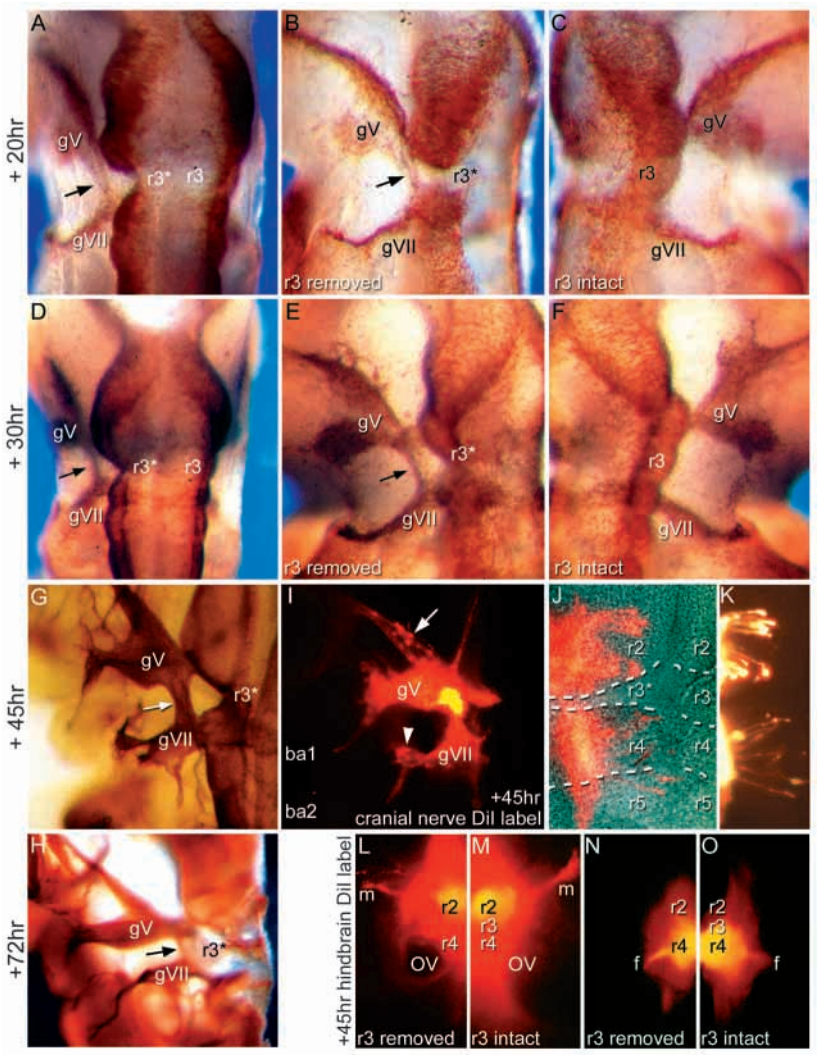

Fig. 6. Aberrant axon pathfinding following r3 removal. Whole-mount anti-neurofilament staining at 20 hours (A-C), 30 hours (D-F), 45 hours (G) or 72 hours (H) after unilateral r3 removal. (A,D) dorsal views, (B,E,G,H) Operated side; (C,F) unoperated side. In each case, an aberrant axon projection was detected within r3* mesenchyme, between the trigeminal (gV) and facial (gVII) ganglia (arrow in A,B,D,E,G,H) and this ectopic cranial nerve grew thicker over time. (I) DiI injection into the ectopic nerve (45 hours after r3 removal) retrogradely labelled sensory neurones within the trigeminal ganglion (arrow) and facial ganglion (arrowhead), while within the hindbrain (J,K) longitudinal sensory axons were labelled, although motor cell bodies in r1/r2 and r4/r5 were not always labelled (J shows combined phase/DiI view of flatmounted hindbrain, K shows DiI view only). Lateral views of embryos after bilateral DiI injections into medial r2 (L,M) or medial r4 (N,O) 45 hours after r3 removal. Anterogradely labelled axons were rarely detected within the ectopic cranial nerve. f, facial nerve; m, mandibular branch of trigeminal nerve; OV, otic vesicle.

Although our data suggest that surface ectoderm and neuroepithelium independently provide patterning cues, there remained the possibility that only one of these tissues was involved. This is because at the most dorsal region of r3 the neuroepithelium and surface ectoderm are closely apposed, and both tissues are likely to be removed in either type of ablation experiment. To address this issue, we performed control experiments in which the most dorsal part of r3 neuroepithelium plus surface ectoderm was unilaterally removed and the embryos processed with *Sox10* riboprobe 20 hours later. No aberrant NCC migration was detected in any of these (6) embryos (not shown), indicating that dorsalmost r3+ectoderm is not sufficient to pattern NCC migration. Moreover, this experiment reveals that, in more ventral locations, where r3 neuroepithelium and r3 surface ectoderm can be separately removed, both of these tissues are required to pattern NCC migration correctly.

DISCUSSION

The segregation of NCCs into three separate streams within the cranial mesenchyme is one of the most striking patterning events in vertebrate head morphogenesis. In this study, we show that the correct segregation of r2 and r4 NCC streams in the chick is enforced, in part, by a NCC-repulsive activity located within r3-adjacent mesenchyme. Previous studies have also suggested that r3 mesenchyme contains a NCC repulsive activity (Farlie et al., 1999; Kuratani and Eichele, 1993; Sechrist et al., 1994), while time-lapse data in the chick (Kulesa and Fraser, 2000) demonstrate that a very few neuroepithelial-derived cells enter r3 mesenchyme during normal development, but

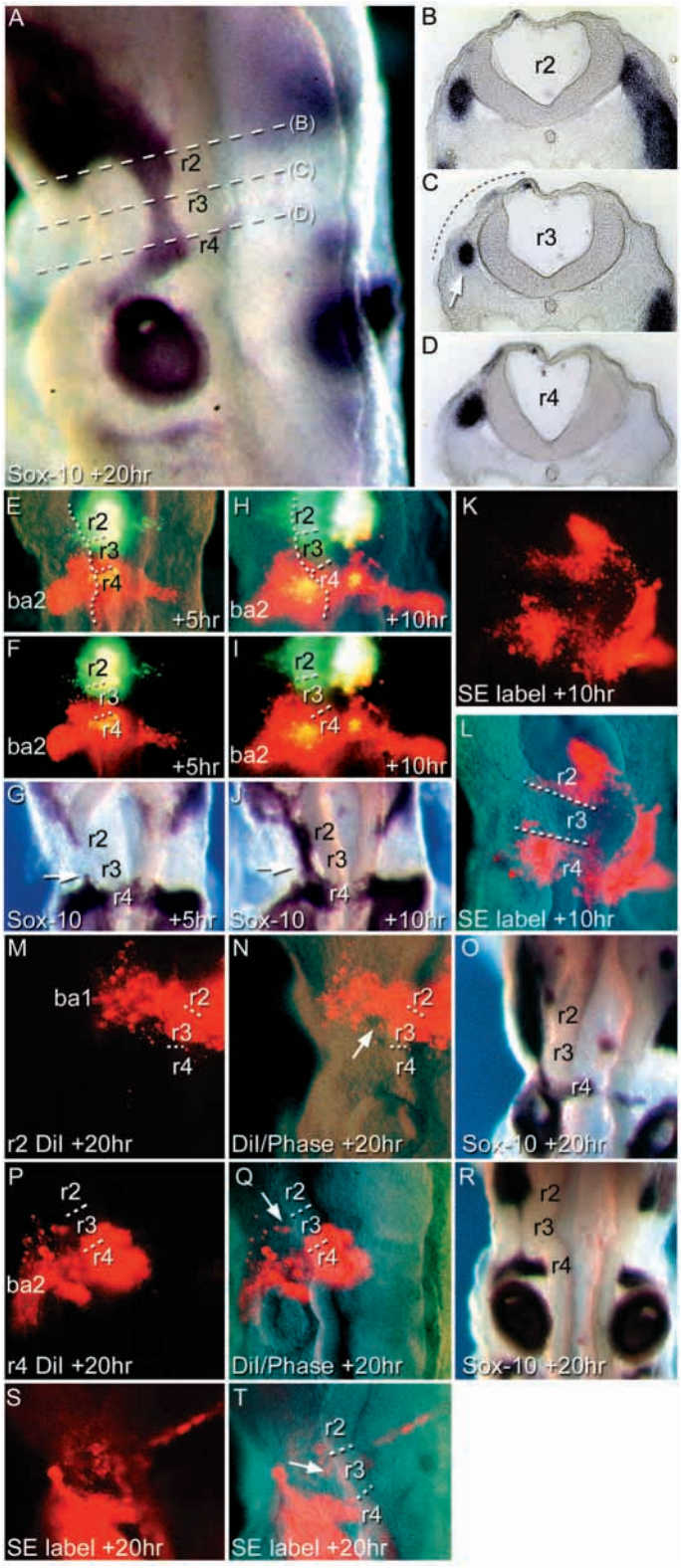

Fig. 7. Altered pattern of cranial NCC migration after surface ectoderm removal. The surface ectoderm overlying r3 was removed unilaterally (left side) and embryos were allowed to develop for a further 20 hours in ovo before *Sox10* in situ hybridisation. (A) A dorsolateral view of the operated side after 20 hours. *Sox10*-expressing NCCs form a robust aberrant projection between the r2 and r4 NCC streams, similar to that seen in r3 removal experiments. (B-D) Serial, slightly oblique, transverse sections through this embryo (broken lines in A show the planes of section in B-D). Arrow in C shows the aberrant NCC projection, while the broken line delineates the dorsoventral extent of surface ectoderm removal. The progression of the phenotype was determined by DiO labelling of dorsal r2 and by DiI labelling of dorsal r4, prior to removal of the r3 surface ectoderm. (E) Combined phase/DiO/DiI dorsal view after 5 hours; (F) DiO/DiI only. Broken lines delineate rhombomere boundaries and outline the neural tube. Some r4 cells (red) deviate rostrally into r3 mesenchyme. (G) A different embryo after 5 hours, revealing some aberrant rostral migration of *Sox10*-expressing r4 NCCs (arrow). (H) Combined phase/DiO/DiI dorsal view after 10 hours; (I) DiO/DiI only. Predominantly, r4 cells (red) enter r3 mesenchyme. (J) A different embryo after 10 hours, showing a bridge of *Sox10*-expressing NCC traversing r3 mesenchyme. (K,L) DiI labelling of surface ectoderm prior to r3 surface ectoderm removal revealed that labelled ectodermal cells had only occasionally re-grown into r3 mesenchyme after 10 hours (L shows combined phase/DiI; broken lines delineate the rostrocaudal extent of surface ectoderm removal). (M-T) Separate r2 DiI labelling and r4 DiI labelling experiments were performed to examine cell migration after 20 hours. (M,N) Several r2 cells migrate aberrantly into r3 mesenchyme (arrow in N). (O) The same embryo processed for *Sox10* in situ reveals a more sharply defined bridge of *Sox10*-expressing NCCs through r3 mesenchyme. (P,Q) Several r4 cells also migrate aberrantly into r3 mesenchyme after 20 hours (arrow in Q). (R) Same embryo processed for *Sox10* in situ reveals a band of NCCs through r3 mesenchyme. (S,T) DiI labelling of surface ectoderm before r3 surface ectoderm removal revealed that several labelled ectodermal cells had re-grown into r3 mesenchyme after 20 hours (arrow), suggesting that the more disperse *Sox10*-negative cells within r3 mesenchyme may be of ectodermal origin (T shows combined phase/DiI). ba1 and ba2, branchial arches 1 and 2.

quickly collapse their filopodia and come to a near standstill or change direction to migrate away from r3 mesenchyme towards the neighbouring r2 or r4 NCC streams. The present study, however, is the first to demonstrate that both neuroepithelium and surface ectoderm at the level of r3 are required to maintain repulsive activities within r3 mesenchyme. We demonstrate how the r3-dependent and surface ectoderm-dependent repulsive activities are temporally regulated and show that in the absence of r3, NCC derivatives persist in ectopic locations for at least 3 days.

NCCs respond heterogeneously to mesenchymal pathfinding cues

Two features of NCC pathfinding are demonstrated by our results. First, the migration of only subpopulations of r2 NCCs and r4 NCCs are affected by our surgical interventions. Second, it is initially mainly r4 NCC migration that is affected by surface ectoderm removal or r3 removal, although the onset of aberrant migration is sooner following surface ectoderm removal. These observations suggest first the existence of multiple NCC repulsive activities in r3 mesenchyme, some of which persist in the absence of neighbouring neuroepithelium and ectoderm, and second, intrinsic differences in responsiveness of r4 NCCs and r2 NCCs to these repulsive activities.

Our results do not allow us to determine which tissues actually synthesise the repulsive activity but as the ectoderm-dependent activity dissipates faster than the neuroepithelial-dependent activity, it is possible that a sequence of signals

needs to be relayed from neuroepithelium to ectoderm to mesenchyme.

An alternative interpretation of the first point is that removal of r3 or r3 ectoderm might make r3 mesenchyme permissive to all NCCs, but adhesive interactions with appropriate NCC pathways (Bronner-Fraser, 1984; Bronner-Fraser, 1985; Bronner-Fraser, 1986; Bronner-Fraser, 1987; Kil et al., 1996) or chemoattraction from target tissues (Kubota and Ito, 2000; Sechrist et al., 1994) exert stronger influences on the migration of most NCCs than the lure of the new territory opened up by the loss of the mesenchymal repulsive activity.

The second point is less contentious, as the intrinsic behavioural differences between r4 NCCs and r2 NCCs revealed by our heterotopic rhombomere transplantation experiments could be related to well-established molecular differences between these populations of migrating NCCs for example in their expression of Hox genes (Hunt et al., 1991; Prince and Lumsden, 1994; Trainor and Krumlauf, 2000a) and *Noggin* (Smith and Graham, 2001).

The observation that aberrantly migrating *Sox10*$^+$ NCCs migrate in a tightly defined dorsolateral pathway raises the possibility that cryptic pathfinding cues might be specified within r3 mesenchyme, but that these are normally masked by the overriding influence of repulsive activities. Intriguingly, the aberrant NCC pathway lies in the same dorsoventral plane as the nerve exit points and cranial ganglia, suggesting that cues for NCC migration or differentiation may be produced by all rhombomeres at this DV level. However, these putative common cues are unlikely to specify exit points, as neither breaks in the neural tube basal lamina nor ectopic *Sox10*$^+$ NCC boundary caps (Niederlander and Lumsden, 1996) were found alongside r3 after surface ectoderm removal (Fig. 7C).

Molecular mechanisms that pattern NCC migration

Several studies have shown alterations in cranial NCC migration or cranial nerve projection in response to respecifying rhombomere identity using retinoic acid or targeted changes in Hox gene expression (Alexandre et al., 1996; Bell et al., 1999; Lee et al., 1995). However, our analysis of *Hoxa2* and *EphA4* expression patterns provides no evidence for respecification of r2 or r4 identity after r3 removal.

Within the hindbrain, Eph/ephrin interactions are important for restricting cell intermixing between rhombomeres (Mellitzer et al., 1999; Xu et al., 1995; Xu et al., 1999). In *Xenopus* embryos Eph/ephrin interactions are also important for regulating cranial NCC migration pathways, as inactivation of these signalling mechanisms (specifically, EphA2, or EphA4, EphB1 and their cognate ligand ephrinB2) leads to ectopic migration of ba3 NCCs (from r5, r6 and r7) into ba2 and ba4 (Helbling et al., 1998; Robinson et al., 1997; Smith et al., 1997). Similarly, in the mouse, loss of ephrinB2 leads to ectopic scattered migration of non-gliogenic r4 NCCs at the level of ba2 (Adams et al., 2001). However, no regional differences in Eph or ephrin expression have been reported in more dorsal regions of cranial mesenchyme adjacent to r2-r4, and inactivation of Eph/ephrin signalling does not result in altered NCC migration patterns similar to those we report here, indicating that other molecules pattern these earlier stages of NCC migration.

One defect in cranial NCC migration that does resemble the phenotype we report here is seen in mice lacking the receptor tyrosine kinase erbB4 (Gassmann et al., 1995; Golding et al., 2000). In these mice, a subpopulation of late-migrating r4 NCCs enter r3 mesenchyme and also contribute to the trigeminal ganglion. Subsequently, an ectopic cranial nerve is produced between the trigeminal and facial/acoustic ganglia. During the period of NCC migration, r3 expresses *Erbb4* in mouse (Gassmann et al., 1995) and chick (Dixon and Lumsden, 1999), suggesting that the similar r3-dependent NCC phenotype we report here could be related to a loss of erbB4-mediated signalling.

In summary, our data reveal that tripartite signalling interactions between neuroepithelium, surface ectoderm and mesenchyme help sculpt the initial pathways taken by migrating cranial NCCs. Future work will attempt to identify these patterning cues and determine whether the repulsive activities within r3 mesenchyme are synthesised locally or are supplied by the neighbouring tissues. Several different signalling systems are probably required to pattern NCC migration correctly within the developing head, and a crucial goal of developmental biology is therefore to determine how these various cues co-operate or integrate with each other to direct head morphogenesis.

We thank Paul Trainor, Hester Tidcombe and Vicky Tsoni for critically reviewing the paper. This work was supported by the Medical Research Council of Great Britain.

Note added in proof

A recent study by Trainor et al. (Trainor et al., 2002) demonstrates that in mouse embryos, the crest-free zone adjacent to r3 is maintained by combinatorial interactions between r3 neuroepithelium and the adjacent mesenchyme/surface ectoderm.

REFERENCES

Adams, R. H., Diella, F., Hennig, S., Helmbacher, F., Deutsch, U. and Klein, R. (2001). The cytoplasmic domain of the ligand ephrinB2 is required for vascular morphogenesis but not cranial neural crest migration. *Cell* **104**, 57-69.

Alexandre, D., Clarke, J. D., Oxtoby, E., Yan, Y. L., Jowett, T. and Holder, N. (1996). Ectopic expression of Hoxa-1 in the zebrafish alters the fate of the mandibular arch neural crest and phenocopies a retinoic acid-induced phenotype. *Development* **122**, 735-746.

Bell, E., Wingate, R. J. and Lumsden, A. (1999). Homeotic transformation of rhombomere identity after localized Hoxb1 misexpression. *Science* **284**, 2168-2171.

Bronner-Fraser, M. (1984). Latex beads as probes of a neural crest pathway; effects of laminin, collagen, and surface charge on bead translocation. *J. Cell Biol.* **98**, 1947-1960.

Bronner-Fraser, M. (1985). Alterations in neural crest migration by a monoclonal antibody that affects cell adhesion. *J. Cell Biol.* **101**, 610-617.

Bronner-Fraser, M. (1986). An antibody to a receptor for fibronectin and laminin perturbs cranial neural crest development in vivo. *Dev. Biol.* **117**, 528-536.

Bronner-Fraser, M. (1987). Perturbation of cranial neural crest migration by the HNK-1 antibody. *Dev. Biol.* **123**, 321-331.

Bronner-Fraser, M. (1995). Origins and developmental potential of the neural crest. *Exp. Cell Res.* **218**, 405-417.

Cheng, Y.-C., Cheung, M., Abu-Elmagd, M. M., Orme, A. and Scotting, P. J. (2000). Chick Sox10, a transcription factor expressed in both early neural crest cells and central nervous system. *Dev. Brain Res.* **121**, 233-241.

Dixon, M. and Lumsden, A. (1999). Distribution of neuregulin-1 (nrg1) and

erbB4 transcripts in embryonic chick hindbrain. *Mol. Cell. Neurosci.* **13**, 237-258.

Eickholt, B. J., Mackenzie, S. L., Graham, A., Walsh, F. S. and Doherty, P. (1999). Evidence for collapsin-1 functioning in the control of neural crest migration in both trunk and hindbrain regions. *Development* **126**, 2181-2189.

Farlie, P. G., Kerr, R., Thomas, P., Symes, T., Minichiello, J., Hearn, C. J. and Newgreen, D. (1999). A paraxial exclusion zone creates patterned cranial neural crest cell outgrowth adjacent to rhombomeres 3 and 5. *Dev. Biol.* **213**, 70-84.

Freund, R., Dorfler, D., Popp, W. and Wachtler, F. (1996). The metameric pattern of the head mesoderm – does it exist? *Anat. Embryol.* **193**, 73-80.

Gassmann, M., Casagranda, F., Orioli, D., Simon, H., Lai, C., Klein, R. and Lemke, G. (1995). Aberrant neural and cardiac development in mice lacking the ErbB4 neuregulin receptor. *Nature* **378**, 390-394.

Golding, J. P., Trainor, P., Krumlauf, R. and Gassmann, M. (2000). Defects in pathfinding by cranial neural crest cells in mice lacking the neuregulin receptor ErbB4. *Nat. Cell Biol.* **2**, 103-109.

Graham, A., Koentges, G. and Lumsden, A. (1996). Neural crest apoptosis and the establishment of craniofacial pattern: an honorable death. *Mol. Cell. Neurosci.* **8**, 76-83.

Grove, E. A., Tole, S., Limon, J., Yip, L.-W. and Ragsdale, C. W. (1998). The hem of the embryonic cerebral cortex is defined by the expression of multiple Wnt genes and is compromised in Gli3-deficient mice. *Development* **125**, 2315-2325.

Guthrie, S., Muchamore, I., Kuroiwa, A., Marshall, H., Krumlauf, R. and Lumsden, A. (1992). Neuroectodermal autonomy of Hox-2.9 expression revealed by rhombomere transpositions. *Nature* **356**, 157-159.

Guthrie, S., Prince, V. and Lumsden, A. (1993). Selective dispersal of avian rhombomere cells in orthotopic and heterotopic grafts. *Development* **118**, 527-583.

Helbling, P. M., Tran, C. T. and Brandli, A. W. (1998). Requirement for EphA receptor signaling in the segregation of Xenopus third and fourth arch neural crest cells. *Mech. Dev.* **78**, 63-79.

Holder, N. and Klein, R. (1999). Eph receptors and ephrins: effectors of morphogenesis. *Development* **126**, 2033-2044.

Holley, J. A. and Yu, R. K. (1987). Localization of glycoconjugates recognized by the HNK-1 antibody in mouse and chick embryos during early neural development. *Dev. Neurosci.* **9**, 105-119.

Hunt, P., Ferretti, P., Krumlauf, R. and Thorogood, P. (1995). Restoration of normal Hox code and branchial arch morphogenesis after extensive deletion of hindbrain neural crest. *Dev. Biol.* **168**, 584-597.

Hunt, P., Wilkinson, D. and Krumlauf, R. (1991). Patterning the vertebrate head – murine Hox-2 genes mark distinct subpopulations of premigratory and migrating neural crest. *Development* **112**, 43-50.

Kil, S. H., Lallier, T. and Bronner-Fraser, M. (1996). Inhibition of cranial neural crest adhesion in vitro and migration in vivo using integrin antisense oligonucleotides. *Dev. Biol.* **179**, 91-101.

Koentges, G. and Lumsden, A. (1996). Rhombencephalic neural crest segmentation is preserved throughout craniofacial ontogeny. *Development* **122**, 3229-3242.

Kubota, Y. and Ito, K. (2000). Chemotactic migration of mesencephalic neural crest cells in the mouse. *Dev. Dyn.* **217**, 170-179.

Kulesa, P. M. and Fraser, S. E. (1998). Neural crest cell dynamics revealed by time-lapse video microscopy of whole chick explant cultures. *Dev. Biol.* **204**, 327-344.

Kulesa, P. M. and Fraser, S. E. (2000). In ovo time-lapse analysis of chick hindbrain neural crest cell migration shows cell interactions during migration to the branchial arches. *Development* **127**, 1161-1172.

Kulesa, P., Bronner-Fraser, M. and Fraser, S. (2000). In ovo time-lapse analysis after dorsal neural tube ablation shows rerouting of chick hindbrain neural crest. *Development* **127**, 2843-2852.

Kuratani, S. C. and Eichele, G. (1993). Rhombomere transplantation repatterns the segmental organisation of cranial nerves and reveals cell-autonomous expression of homeodomain protein. *Development* **117**, 105-117.

Le Douarin, N. M. (1982). *The Neural Crest*. Cambridge: Cambridge University Press.

Lee, Y. M., Osumi-Yamashita, N., Ninomiya, Y., Moon, C. K., Eriksson, U. and Eto, K. (1995). Retinoic acid stage-dependently alters the migration pattern and identity of hindbrain neural crest cells. *Development* **121**, 825-837.

Lumsden, A. and Keynes, R. (1989). Segmental patterns of neuronal development in the chick hindbrain. *Nature* **337**, 424-428.

Lumsden, A. and Krumlauf, R. (1996). Patterning the vertebrate neuraxis. *Science* **274**, 1109-1115.

Lumsden, A., Sprawson, N. and Graham, A. (1991). Segmental origin and migration of neural crest cells in the hindbrain region of the chick embryo. *Development* **113**, 1281-1291.

Maden, M., Hunt, P., Eriksson, U., Kuroiwa, A., Krumlauf, R. and Summerbell, D. (1991). Retinoic acid-binding protein, rhombomeres and the neural crest. *Development* **111**, 35-43.

Mason, I. (1999). Chick embryos: incubation and isolation. In *Methods in Molecular Biology*. Vol. 97 (ed. P. T. Sharpe and I. Mason), pp. 221-224. Totowa, NJ: Humana Press.

Mellitzer, G., Xu, Q. and Wilkinson, D. (1999). Eph receptors and ephrins restrict cell intermingling and communication. *Nature* **400**, 77-81.

Niederlander, C. and Lumsden, A. (1996). Late emigrating neural crest cells migrate specifically to the exit points of cranial branchiomotor nerves. *Development* **122**, 2367-2374.

Nieto, M. A., Gilardi-Hebenstreit, P., Charnay, P. and Wilkinson, D. A. (1992). A receptor protein tyrosine kinase implicated in the segmental patterning of the hindbrain and mesoderm. *Development* **116**, 1137-1150.

Prince, V. and Lumsden, A. (1994). Hoxa-2 expression in normal and transposed rhombomeres: independent regulation in the neural tube and neural crest. *Development* **120**, 911-923.

Robinson, V., Smith, A., Flenniken, A. M. and Wilkinson, D. G. (1997). Roles of Eph receptors and ephrins in neural crest pathfinding. *Cell Tissue Res.* **290**, 265-274.

Sechrist, J., Scherson, T. and Bronner-Fraser, M. (1994). Rhombomere rotation reveals that multiple mechanisms contribute to segmental pattern of hindbrain neural crest migration. *Development* **120**, 1777-1790.

Sechrist, J., Serbedzija, G. N., Scherson, T., Fraser, S. E. and Bronner-Fraser, M. (1993). Segmental migration of the hindbrain neural crest does not arise from its segmental generation. *Development* **118**, 691-703.

Smith, A. and Graham, A. (2001). Restricting Bmp-4 mediated apoptosis in hindbrain neural crest. *Dev. Dyn.* **220**, 276-283.

Smith, A., Robinson, V., Patel, K. and Wilkinson, D. G. (1997). The EphA4 and EphB1 receptor tyrosine kinases and ephrin-B2 ligand regulate targeted migration of branchial neural crest cells. *Curr. Biol.* **7**, 561-570.

Trainor, P. and Krumlauf, R. (2000a). Patterning the cranial neural crest: hindbrain segmentation and Hox gene plasticity. *Nat. Rev. Neurosci.* **1**, 116-124.

Trainor, P. and Krumlauf, R. (2000b). Plasticity in mouse neural crest cells reveals a new patterning role for cranial mesoderm. *Nat. Cell Biol.* **2**, 96-102.

Trainor, P. A., Sobieszczuk, D., Wilkinson, D. and Krumlauf, R. (2002). Signalling between the hindbrain and paraxial tissues dictates neural crest migration pathways. *Development* **129**, 433-442.

Xu, Q., Alldus, G., Holder, N. and Wilkinson, D. G. (1995). Expression of truncated Sek-1 receptor tyrosine kinase disrupts the segmental restriction of gene expression in the Xenopus and zebrafish hindbrain. *Development* **121**, 4005-4016.

Xu, Q., Mellitzer, G., Robinson, V. and Wilkinson, D. (1999). In vivo cell sorting in complementary segmental domains mediated by Eph receptors and ephrins. *Nature* **399**, 267-271.